Available online at www.sciencedirect.com

ScienceDirect

Energy Procedia 4 (2011) 4747–4753

Energy Procedia

www.elsevier.com/locate/procedia

GHGT-10

Geochemical evaluation of CO_2 injection into storage reservoirs based on case-studies in The Netherlands

Tim Tambach[1*], Mariëlle Koenen, and Frank van Bergen

TNO Geological Survey of The Netherlands, P.O. Box 80015, 3508 TA Utrecht, The Netherlands

Abstract

Over the past few years several geochemical evaluations of CO_2 storage in Dutch potential reservoirs are carried out, including predictions of the short- and long-term impact of CO_2 on the reservoir using geochemical modelling. The initial mineralogy of the reservoir is frequently obtained from core analysis and is then used to compute the formation water composition. In this paper geochemical modelling with *TOUGHREACT* is used to predict and compare the short- and long-term geochemical impact of CO_2 injection into three reservoirs. The mineralogical composition of these reservoirs is an assemblage based on commonly observed minerals from the Buntsandstein and Rotliegend formations. These formations contain potential onshore and offshore CO_2 storage locations in the Netherlands. The results predict drying out and salt precipitation in the near-well area, due to water evaporation by the injected dry CO_2. Several mineral transformations are predicted, dominated by the transformation of albite into dawsonite, thereby fixing CO_2. Due to the relatively low density of dawsonite, the porosity significantly decreases, which can lead to a pore pressure increase. Disabling of dawsonite precipitation in the simulations, thereby taking into account the ongoing debate on dawsonite stability, only shows a small increase of the porosity. Future (experimental) work should be focused on dawsonite occurrence for accurate predictions of the long-term reservoir integrity.

Keywords: CO_2 storage; geochemistry; geochemical modelling; dawsonite; CCS

1. Introduction

The Netherlands play a key role in the implementation of CCS in northwestern Europe. Relatively large storage capacity is available, distances between CO_2 sources and storage reservoirs are relatively short, and infrastructure for (cross-border) gas transport over large distances is already installed. Application of CCS within the next 5 years is promoted in the Netherlands and there is strong commitment to reach the emission reductions. Oil and gas production from Dutch reservoir is maturing and the expectation is that many fields will be abandoned in the coming two decades. CCS should be applied within the same period or shortly after, to benefit from the use of (adapted) existing infrastructure such as platforms, wells, and pipelines.

* Corresponding author. Tel.: +31-30-2564793; fax: +31-30-2564605
E-mail address: tim.tambach@tno.nl

doi:10.1016/j.egypro.2011.02.438

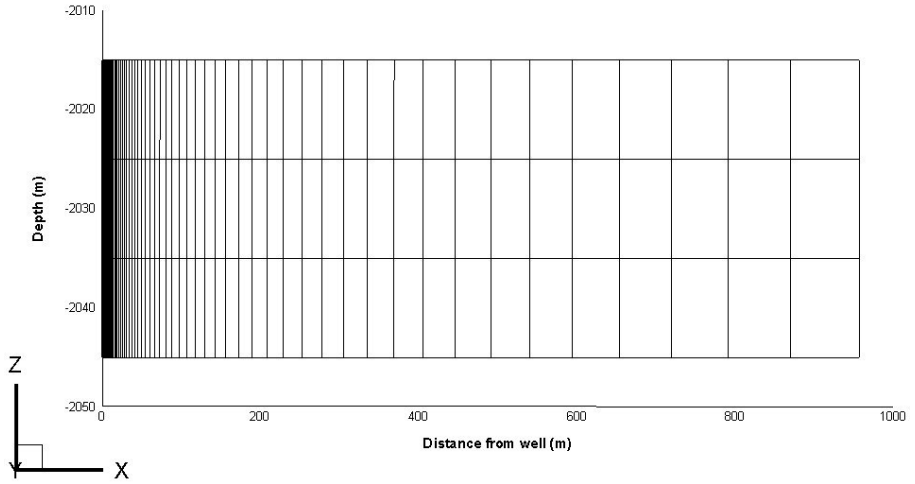

Figure 1: 2D window (cell-centered) of the radial model containing four layers of 100 grid cells. Near-well effects are taken into account by defining fine grid cells close to the well.

Several oil and gas fields in the subsurface of the Netherlands are currently evaluated as potential location for CO_2 storage, for example K12-B in the offshore part of the Netherlands (Van der Meer et al., 2005; Audigane et al., 2008). There is a need for finding a clear and consistent methodology to support policy makers and field operators to evaluate the short-term operational effects and long-term containment of CO_2 storage in the reservoir. One of the important aspects is the geochemical response of the potential storage reservoir upon CO_2 injection, as shown by several case studies of potential CO_2 storage sites (Xu et al., 2004; Gaus et al., 2005; Audigane et al., 2008; Tambach et al., 2009). The predicted geochemical effects are not known for causing potential delays of worldwide CO_2 storage projects, although geochemical modelling, especially long-term, has many uncertainties (Gaus, 2010).

In The Netherlands the main CO_2 storage capacity is expected in Permian Rotliegendes reservoirs, Triassic Buntsandstein reservoirs, and Cretaceous Rijnland reservoirs. In such reservoirs the mineralogy is dominated by quartz, usually reaching more than 60 wt%. Other minerals that are present consist of feldspars (plagioclase, orthoclase etc.), carbonates (calcite, dolomite etc.), and clay minerals (smectite, illite, kaolinite etc.). The pore space of the reservoir is filled with formation water (brine) and gas, with gas saturations varying from 50% to 85%. The composition of the gas phase predominantly consists of methane (CH_4), but may also contain N_2, CO_2, and higher alkanes. The brine contains high concentrations of dissolved halite (NaCl) and it is commonly assumed that over geological time thermodynamic equilibrium is established between the formation water, the reservoir mineralogy, and the gas phase.

In this paper a possible methodology is discussed, as well as the results of geochemical modelling of CO_2 injection into three sandstone reservoirs. The mineralogy of these sandstones is not directly related to specific locations or case studies, but are simplified representations for potential reservoirs in The Netherlands, as discussed above. The number of primary minerals is limited and is systematically increased for better understanding of the mineral transformations and associated effects. A selection of secondary (precipitating) minerals is specified, including the mineral dawsonite. The ongoing debate on the stability of this mineral is taken into account by disabling it in one of the simulations.

Table 1: Mineralogical composition (volume %) of three sandstone reservoirs, resembling the mineralogy of offshore gas fields in the Netherlands. Magnesium and calcium bearing minerals are only considered in Reservoir B and C. Precipitation of dawsonite is not considered in reservoir C', thereby taking into account the ongoing debate on dawsonite stability (Gaus, 2010).

		Volume fraction			
Mineral	Chemical formula	Reservoir A	Reservoir B	Reservoir C	Reservoir C'
Quartz	SiO_2	0.72	0.64	0.60	0.60
Albite	$NaAlSi_3O_8$	0.04	0.04	0.04	0.04
K-feldspar	$KAlSi_3O_8$	0.04	0.04	0.04	0.04
Dolomite	$CaMg(CO_3)_2$	-	0.08	0.08	0.08
Illite	$K_{0.6}Mg_{0.25}Al_{2.3}Si_{3.5}O_{10}(OH)_2$	-	-	0.04	0.04
Porosity		0.20	0.20	0.20	0.20
Secondary (precipitating) minerals considered:					
Dawsonite		+	+	+	-
Diaspore, Kaolinite, Muscovite, Pyrophyllite, Paragonite		+	+	+	+
Anorthite, Calcite, Magnesite, Oligoclase, Montmorillonite(Ca,K,Mg,Na), Smectite(Ca,K,Mg,Na)		-	+	+	+

2. Simulation details

2.1. Reservoir description and CO_2 injection

A radial (R,Z) reservoir model was used with depth of 2010 m, a radius of 1,000 m, and a thickness of 40 m (see Figure 1). Four layers of 100 grid cells are imposed with grid refinement close to the well and dimensions ranging from 7.0×10^{-3} m to 91 m in the R-direction. A porosity of 20% was defined for the reservoir, giving a total pore volume of 2.51×10^{7} m^3 for the full radial model. The irreducible water content is defined as 15%, which is too low for water flow (relative permeability of 0) and describes full gas flow (relative permeability of 1.0). It is reasonable to ignore the influence of mineral dissolution and precipitation on the flow, thereby speeding up the simulations significantly. The model has no-flow boundaries, representing impermeable layers and bounding faults surrounding the reservoir. The permeability is 100 mD in all three directions, and no faults are present in the reservoir. The temperature is 70°C and the initial pressure is 30.0 bars. The initial gas composition consists exclusively of CO_2, as given by the ECO2N module in TOUGHREACT, which describes the interactions between brine and CO_2. The CO_2 is injected with a rate of 10 kg/s (0.32 Mton/year) for 41.5 years, followed by a shut-in of the well. The simulations were continued up to 100,000 years to study the long-term geochemical effects of CO_2 injection. Reference cases, without perturbations such as CO_2 injection, were also computed to account for mineral reactions in the reservoir.

2.2. Reservoir mineralogy

In many case studies the measured mineralogical composition was used, as for example illustrated in a recent paper (Tambach et al., 2009). In the current paper we use simplified models that represent the mineralogical characteristics of reservoirs in the Netherlands. The mineralogy of the reservoirs that we study predominantly consists of quartz and includes K-feldspar and albite (reservoir A). As we are interested in the effects of individual minerals present, we then extend the reservoir with other minerals. This includes dolomite (reservoir B) and dolomite and illite (reservoir C). Geochemically, these reservoirs are more complex than reservoir A, as Ca and Mg are also included. None of the three reservoirs contains iron and sulphate, which will be part of future work. An overview of the mineralogical composition of the reservoir, as used in the simulations, is given in Table 1. The table also includes the selection of common secondary minerals that are allowed to precipitate. Kinetic constants for most mineral precipitation and dissolution reactions were taken from the literature (Palandri and Kharaka., 2004), while calcite precipitation is assumed to be instantaneous.

2.3. Formation water

After definition of the reservoir mineralogy the composition of the formation water needs to be defined before starting the computations on a reservoir scale. The formation water composition is computed from the reservoir mineralogy and thermodynamic equilibrium is assumed. The most important advantage of computing the formation water, rather than using experimental measurements, is that the actual simulations will then start from a well-defined and reproducible initial situation. Experimentally measured formation water compositions will not be in equilibrium with the measured reservoir mineralogy once supplied to and modelled with geochemical software. In such cases the judgement of the user on defining the initial (equilibrium) situation may then contain subjective elements. Furthermore, downhole formation water samples are quite often not available for specific sites and very expensive to retrieve. If they are available they may contain contamination from, for example, drilling muds. Degassing of dissolved CO_2 during sampling and storing may influence the measured pH. Thoughts about the experimentally measured formation water were also brought up by others (Gaus et al., 2005; Audigane et al., 2008). It can, on the other hand, also be discussed whether the simulations should start from thermodynamic equilibrium, as thin sections may show that specific minerals are covered by other minerals or occur as mineral inclusions, thereby (temporally) limiting their accessibility (Peters, 2009). In addition to this, the measured reservoir mineralogy composition may not represent an equilibrium situation as slow transformation of clay minerals, for example, is still ongoing. Despite these considerations, the thermodynamic equilibrium starting point is used here for clarity and reproducibility.

Below the workflow is described for computing the formation water composition in thermodynamic equilibrium with the defined reservoir using *TOUGHREACT* and a relatively basic equation of state (EOS1):

a) Only one grid block (no flow) with the initial mineralogy (no secondary precipitating minerals) is defined. Kinetic parameters are not necessary, as the thermodynamic equilibrium is computed.
b) All the pores are completely filled with brine (c_{brine} = 100 g/l), defining the Na^+ and Cl^- concentrations, while the concentrations of other primary species are defined as negligibly small.
c) A background partial pressure of CO_2 (P_{CO2}=0.1 bar) is defined in addition to the temperature (T) and total pressure (P) in the reservoir.

The equilibrium formation water compositions were computed for all reservoirs mentioned in Table 1. The results were then used in all 400 grid cells of the upscaled 2D radial model, as given in Figure 1.

3. Results

3.1. Short-term effects

The quantitative effects of pressure increase, drying-out and salt precipitation in the near-well area are quite similar for all three reservoirs. During the period of CO_2-injection (i.e. 41.5 years) the pressure steadily increases to approximately 200 bars and the occurrence of mineral transformations is computed to be negligible at this time-scale. The initial water saturation in the pores is 15%. Water evaporates in the dry CO_2 gas stream during injection, leading to a dry-out area in the vicinity of the well-bore. This is illustrated in Figure 2, showing the gas saturation (S_g) as a function of the distance to the wellbore. After shut-in of the well, only marginal changes are encountered. The results show a drying-out front that is increasing over time, with a final radius of 96.8 m. This radius is a direct function of the total amount of CO_2 injected, porosity, initial water saturation, temperature, and (final) pressure. After a relatively small transition zone, the gas saturation is computed to remain constant ($S_g \approx 0.848$) in the remainder of the reservoir up to 1000 m away from the well. The amount of salt that precipitates in the dried out area takes up approximately 0.5% of the total pore volume, which is much less than recently computed for saline aquifers (i.e. 9.1%) by Pruess and Muller (2009). The reason for this difference is that more water and hence more salt is present in saline aquifers.

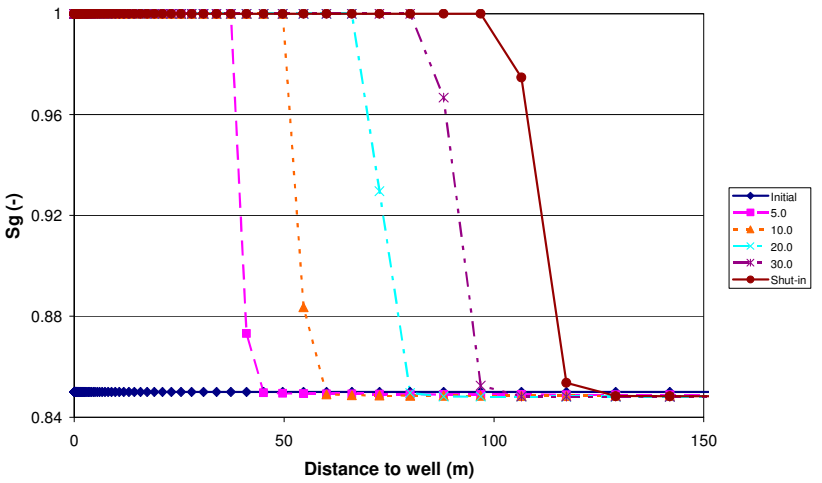

Figure 2: Gas saturation (S_g) or drying out front as a function of the distance to the well during the CO_2 injection into the reservoir (similar for all reservoirs defined in Table 1), after 5, 10, 20, and 30 years. After an injection period of 41.5 years the well is shut-in and the gas saturation does not change significantly. Salt precipitation occurs in the drying out area.

3.2. Long-term effects

Mineral transformation occurs with time, even without the presence of CO_2, caused by slow reacting minerals in the reservoir. The computed changes in volume fraction of dissolving and precipitating minerals in reservoir C, as a result of CO_2 injection and re-equilibration, are shown in Figure 3. The most dominant reaction is the conversion of albite into dawsonite, but transformation of a small amount of K-feldspar into illite is also predicted. Negligible amounts of dolomite and calcite dissolve and precipitate, respectively. Compared to the reference cases without CO_2 injection (fixed background partial pressure of 0.1 bar), feldspar dissolution and illite precipitation (reservoir B and C) is faster. Alteration of K-feldspar depends on the pH and on the activity of dissolved silica and potassium (Gardner, 1972; Deer et al., 2001). Given the conditions of Bunter sandstone reservoirs it is likely that K-feldspar is transformed into alumina silicates, such as kaolinite, pyrophyllite, mica, illite, and muscovite. In this study it is computed that illite is the dominant transformation product for reservoirs B, C, and C' (using Mg^{2+} from dolomite dissolution), while small amounts of muscovite, kaolinite, and pyrophillite are formed in case of reservoir A (no Mg^{2+} present). Small amounts of kaolinite and pyrophillite are also formed together with illite in the absence of dawsonite (reservoir C'). In dissolution experiments, K-feldspar transformation into illite was observed at decreasing pH for temperatures higher than 150°C, while kaolinite is usually dominant at lower temperatures (Meunier and Velde, 2004).

In Figure 4 we show the computed volume fractions of albite and dawsonite as a function of time, as well as the porosity. The results for the reservoirs A, B, and C are quite similar. It is predicted that albite is almost completely transformed into dawsonite, with an associated porosity decrease from 20% to approximately 19.0% (corresponding to a 5.0% reduction of the pore volume) after 100,000 years. This is related to the relatively low density of dawsonite of approximately 2.42 g/cm^3, compared to a density of 2.56 g/cm^3 for K-feldspar. The pressure may increase due to the reduction of pore volume, assuming no effect of pressure on the geochemical reactions. Figure 4 also shows that disabling of dawsonite precipitation (reservoir C') leads to a marginal porosity increase to about 20.1%. Although dawsonite has been observed in some natural analogues (Worden, 2006; Gao et al., 2009) it is not found in other analogues, probably suggesting much lower kinetic reaction rates than currently measured and applied in geochemical modelling (Gaus, 2010). Albite transformation into dawsonite (or any other secondary phase) was not observed in experiments by Hangx and Spiers (2009), most probably due to relatively short reaction times in the order of weeks. The results presented here do not take into account porosity reduction as a result of geomechanical compaction, which will be part of future study.

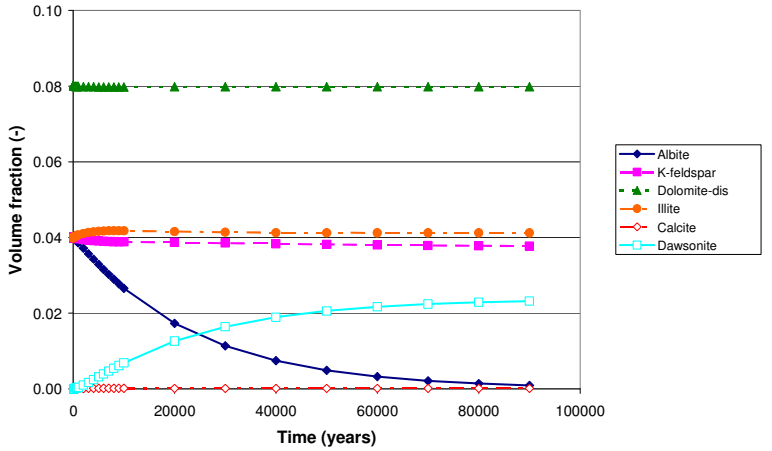

Figure 3:Volume fractions of the minerals in reservoir C as a function of time, representing the reservoir area that is not dried out. The volume fraction of quartz is one order of magnitude higher and therefore not shown.

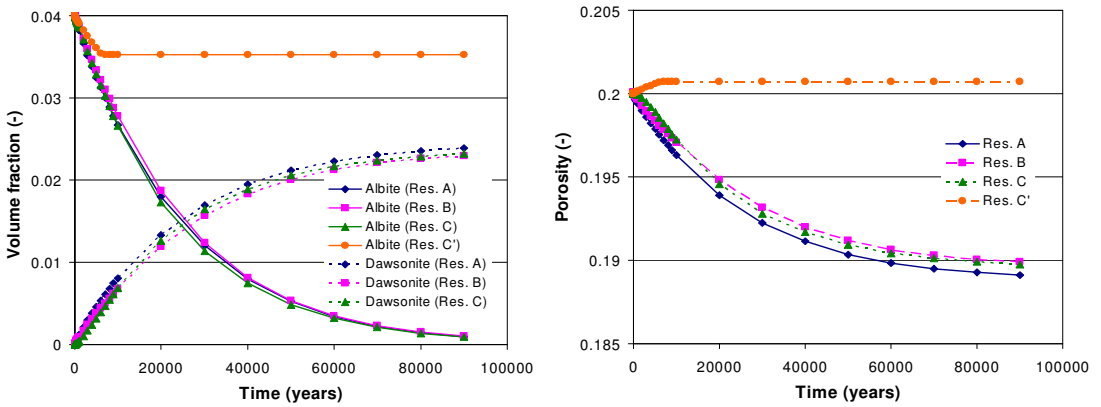

Figure 4: Volume fractions of albite (all reservoirs) and dawsonite (reservoir A, B, and C) as function of time (left) and the porosity as a function of the time for all reservoirs (right). The results represent the reservoir area that is not dried out.

4. Conclusions

This paper reports computations of the geochemical impact of CO_2 injection into three sandstone reservoirs, containing several primary minerals and allowing secondary minerals to precipitate. A workflow for defining the formation water, before injecting CO_2, is discussed. The simulation results of CO_2 injection into the reservoirs show that the near-well area is dried out by water evaporation into the dry CO_2 stream, leading to salt precipitation and a small reduction in the porosity. The transformation of albite into dawsonite is the most predominant reaction, thereby fixing CO_2 and leading to a reduction of the porosity. The transformation of K-feldspar into illite is less predominant, while other mineralogical changes are almost negligible. The low density of dawsonite is predominantly responsible for the computed reduction in porosity, as shown by disabling dawsonite precipitation in an additional run. As the stability of dawsonite is still under debate, it is recommended to focus future work on this topic.

5. References

Audigane, P., Lions, J., Gaus, I., Robelin, C., Durst, P., Oldenburg, C.M., Xu, T., Meer, B.v.d., Geel, K. (2008) Geochemical modelling of CO_2 injection into a methane gas reservoir at the K12-B field, North Sea. In *Carbon dioxide sequestration in geological media - State of the science*. Grobe, M., Pashin, J.C., and Dodge, R.L. (eds): AAPG Studies 59, pp. 1-20.

Deer, W.A., Zussman, J., Howie, R.A., 2001. Rock-forming minerals: Framework silicates: feldspars, Volume 4B. London, Geological Society of London.

Gao, Y.Q., Liu, L., Hu, W.X., 2009. Petrology and isotopic geochemistry of dawsonite-bearing sandstones in Hailaer basin, northeastern China. Applied Geochemistry 24, p. 1724-1738.

Gardner, L.R., 1972. Conditions for direct formation of gibbsite from K-feldspar - Further discussion. American Mineralogist 57, p. 294-300.

Gaus, I., 2010. Role and impact of CO_2-rock interactions during CO_2 storage in sedimentary rocks. International Journal of Greenhouse Gas Control 4, p. 73-89.

Gaus, I., Azaroual, M., Czernichowski-Lauriol, I., 2005. Reactive transport modelling of the impact of CO_2 injection on the clayey cap rock at Sleipner (North Sea). Chemical Geology 217, p. 319-337.

Hangx, S.J.T., Spiers, C.J., 2009. Reaction of plagioclase feldspars with CO_2 under hydrothermal conditions. Chemical Geology 265, p. 88-98.

Meunier, A., Velde, B., 2004. Illite: origins, evolution, and metamorphism. Berlin, Springer.

Palandri, J., Kharaka., Y.K., 2004. A compilation of rate parameters of water-mineral interaction kinetics for application to geochemical modelling. US Geological Survey Open File Report 2004-1068, USGS.

Peters, C.A., 2009. Accessibilities of reactive minerals in consolidated sedimentary rock: An imaging study of three sandstones. Chemical Geology 265, p. 198-208.

Pruess, K., Muller, N., 2009. Formation dry-out from CO_2 injection into saline aquifers: 1. Effects of solids precipitation and their mitigation. Water Resources Research 45.

Tambach, T.J., Benedictus, T., Van Bergen, F., Vandeweijer, V.P., Van der Meer, L.G.H., 2009. A geochemical study of CO_2 injection into depleted gas fields in The Netherlands. Lawrence Berkeley National Laboratory, U.S.A.

Van der Meer, L.G.H., Kreft, E., Geel, C., Hartman, J., 2005. K12-B a Test Site for CO_2 Storage and Enhanced Gas Recovery. SPE 94128.

Worden, R.H., 2006. Dawsonite cement in the Triassic Lam Formation, Shabwa Basin, Yemen: A natural analogue for a potential mineral product of subsurface CO_2 storage for greenhouse gas reduction. Marine and Petroleum Geology 23, p. 61-77.

Xu, T., Apps, J.A., Pruess, K., 2004. Numerical simulation of CO_2 disposal by mineral trapping in deep aquifers. Applied Geochemistry 19, p. 917-936.